Front. Chem. Sci. Eng. 2021, 15(4): 872–881
https://doi.org/10.1007/s11705-020-2001-2

RESEARCH ARTICLE

Recovery of free volume in PIM-1 membranes through alcohol vapor treatment

Faiz Almansour[1], Monica Alberto[1], Rupesh S. Bhavsar[2], Xiaolei Fan[1], Peter M. Budd[2], Patricia Gorgojo (✉)[1]

1 Department of Chemical Engineering and Analytical Science, School of Engineering, The University of Manchester, Manchester M13 9PL, UK
2 Department of Chemistry, School of Natural Sciences, The University of Manchester, Manchester M13 9PL, UK

Abstract Physical aging is currently a major obstacle for the commercialization of PIM-1 membranes for gas separation applications. A well-known approach to reversing physical aging effects of PIM-1 membranes at laboratory scale is soaking them in lower alcohols, such as methanol and ethanol. However, this procedure does not seem applicable at industrial level, and other strategies must be investigated. In this work, a regeneration method with alcohol vapors (ethanol or methanol) was developed to recover permeability of aged PIM-1 membranes, in comparison with the conventional soaking-in-liquid approach. The gas permeability and separation performance, before and post the regeneration methods, were assessed using a binary mixture of CO_2 and CH_4 (1:1, v:v). Our results show that an 8-hour methanol vapor treatment was sufficient to recover the original gas permeability, reaching a CO_2 permeability > 7000 barrer.

Keywords polymer of intrinsic microporosity (PIM), PIM-1, physical aging, gas separation, vapor-phase regeneration

1 Introduction

Since the commercialization of the first membrane-based system for gas separation applications three decades ago, a wide range of polymers have been investigated and developed, but less than ten have made it to commercial use [1]. Non-network polymer of intrinsic microporosity (PIM-1), synthesized for the first time at the University of Manchester two decades ago [2], has shown great potential as a membrane material at laboratory scale, due to its high chemical, thermal and mechanical stability, as well as high gas permeability (arising from its high free volume) and fair selectivity values. All these properties also make it attractive for commercial gas separation applications [3,4]. However, as generally happens to high free volume polymers, PIM-1 is prone to lose the void space rapidly due to physical aging, which results in the loss of membrane performance over time. The polymer chains are initially packed in a non-equilibrium state, leaving excess free volume. Over time, loss of free volume occurs by the gradual rearrangement of the polymer chains towards an equilibrium state, leading to an increase of polymer density. As a consequence the permeability of the membrane is reduced, compromising its long-term stability. This effect is more pronounced at the beginning of its lifetime, with a significant decline in permeability, the rate of which decreases with time [5,6]. Similarly to other polymers [7], the rate of physical aging in PIM-1 membranes is also thickness-dependent, being faster in thin films compared to thicker films [8,9]. Other factors, such as temperature, pressure, atmosphere and storage conditions, also play an important role in the physical aging rate [10–12].

It is worth noting that several other solution-processable PIMs synthesized over the past few years have overcome the well-known Robeson 2008 upper bound for certain gas pairs [13,14]. However, as with PIM-1, they also suffer from physical aging [15–17], and PIM-1 is still the most investigated non-network PIM. Different approaches have been explored to prevent or minimize physical aging in PIM-1 membranes, including: 1) modification and synthesis of new polymer structures [6,18], 2) post-modification treatments (e.g., thermal oxidative crosslinking [19], the use of supercritical CO_2, and ultraviolet treatment [20]), and 3) addition of fillers to the polymer matrix, giving so-called mixed matrix membranes [21–23]. Physical aging is a reversible process, unlike others such as degradation, chemical aging and contamination that affect membrane properties irreversibly [1]. In some glassy polymers, such as polysulfone and polyimide, the membrane performance

Received June 24, 2020; accepted August 3, 2020

E-mail: p.gorgojo@manchester.ac.uk

is recovered by annealing the sample above its glass transition temperature (T_g), followed by rapid quenching to room temperature [24]. However, in polymers with very high or undetectable T_g, the group to which PIM-1 belongs, this is not possible [1]. In this case, the 'rejuvenation' of the membrane performance is typically undertaken by soaking the films in lower alcohols, such as methanol or ethanol [8,12,13,25]. Alcohols swell PIM-1, causing an enhancement of the molecular motion of the polymer chains that leads to an increase in the free volume of the polymer [26]. In addition, the alcohol treatment also flushes out any residual solvents and contaminants trapped within the polymer and erases the past processing history [12]. Similarly, other studies have reported the post-treatment of membranes with a range of solvents to enhance their performance in applications such as organic solvent nanofiltration [27,28], reverse osmosis [29], nanofiltration [30], ultrafiltration [31,32] and pervaporation [33].

Albeit soaking in alcohol is a simple procedure, which is typically done after membrane casting, it requires the removal of the membrane from the gas separation apparatus when it is used to recover permeability of aged membranes. This might be acceptable for small scale and fundamental studies, however, at the industrial level, this procedure would be completely unattainable; membrane modules used in gas separation are not designed to cope with liquid, and a treatment that does not require membrane dismantling would be desirable. Moreover, we envisage that the treatment with alcohol vapor would not cause any further disturbance in the gas separation system, and the use of an inert gas or air following the vapor treatment could eliminate any traces of alcohol vapor and leave the membrane module ready to use. Therefore, in this work we present an alternative that consists in exposing aged PIM-1 films to ethanol or methanol vapor four months after casting, measuring their gas permeability before and after the alcohol treatment as a means of tracking recovery of free volume. One of the most promising applications of PIM-1 membranes at commercial scale is the sweetening of natural gas. Therefore, the separation of the relevant gas pair CO_2/CH_4 was investigated.

2 Experimental

2.1 Materials

Potassium carbonate (K_2CO_3) and 2,3,5,6-tetrafluoroterephthalonitrile (TFTPN) were purchased from Sigma-Aldrich (UK). 3,3,3′,3′-Tetramethyl-1,1′-spirobisindane-5,5′,6,6′-tetraol (TTSBI) was purchased from Alfa Aesar (UK). Dimethylacetamide, dichloromethane, chloroform, toluene, acetone, methanol ($\geqslant$99.5%) and ethanol ($\geqslant$99.5%) were purchased from Sigma-Aldrich (UK). TFTPN was purified by sublimation at 150 °C and then collected without vacuum. TTSBI was dissolved in methanol and precipitated in dichloromethane before use. All the other chemicals were used as received.

2.2 Synthesis of PIM-1

PIM-1 was synthetized following the procedure proposed by Du et al. [34]. Firstly, 10.00 g of TFTPN, 17.29 g of TTSBI and 20.73 g of K_2CO_3 were reacted in a mixed solvent of 100 mL of dimethylacetamide and 50 mL of toluene under N_2 at 160 °C. Reflux and constant mechanical stirring of the solution was set for 40 min, after which a highly viscous solution was produced. This solution was soaked in methanol and left overnight. The yellow crude product was collected by vacuum filtration and washed three times with methanol and a final wash with acetone. Then, it was dissolved in chloroform and re-precipitated in methanol. The recovered product was refluxed for 12 h in water at 100 °C and then dried under vacuum at 110 °C overnight.

2.3 Fabrication of membranes

Thirteen freestanding PIM-1 membranes were prepared through a solvent evaporation method. First, the synthesized PIM-1 powder was dissolved in chloroform at a concentration of 4 wt-% under magnetic stirring for 24 h. Then, the dope solution was cast on Steriplan® petri dishes (5 cm diameter) that were immediately covered and left in the fume cupboard for 3 d at room temperature. The thickness of the membranes was measured using a digital micrometer screw gauge with an accuracy of $\pm$0.5 μm (Mitutoyo IP65 Coolant Proof, UK). At least five measurements were performed on each membrane to obtain an average thickness.

2.4 Membrane treatment

From the prepared PIM-1 membranes, three were tested without any alcohol treatment and were labelled as PIM-1 as-cast (Table 1). The rest were subjected to treatment with methanol or ethanol the day after collection from the petri dish (day 1). For the treatment, membranes were immersed in alcohol for 24 h at room temperature, and subsequently placed in a vacuum oven at 120 °C for 10 h to remove any trapped residual solvents. Further treatment with alcohol vapor was carried out for two of the ethanol-treated membranes and two of the methanol-treated ones, using the same vaporized alcohol as that in the initial solvent treatment. PIM-1 membranes were placed in a membrane cell and exposed to the alcohol vapor generated by the heating of either ethanol or methanol at 50 °C. A vacuum of 10 mbar was applied on the downstream side of the membrane in order to force the passage of the alcohol vapor across the membrane. This procedure is illustrated in

Table 1 CO_2 permeability and CO_2/CH_4 selectivity of fresh and aged PIM-1 membranes

Membrane code	Aging time/d	CO_2 Permeability/barrer	Selectivity (α_{CO_2/CH_4})	Average thickness/μm
PIM-1 (as-cast)[a)]	2	2755±137	18.1±4.2	(39±1) (35±3) (44±3)
PIM-1-MeOH-L(1)[a)]	1	6272±142	12.1±1.0	(34±2) (30±5) (36±3)
	26	3810±868	18.1±4.0	(41±2) (40±4) (43±4)
PIM-1-EtOH-L(1)[a)]	2	4513±1228	19.1±1.4	(48±4) (56±5) (53±3)
	27	3217±614	22.6±2.7	(53±6) (47±9) (51±8)
PIM-1-MeOH-L(1)-V(120)-a	4	6314	11.8	34±4
	26	4432	13.9	
	92	3067	17.9	
	118	2732	20.7	
	121[b)]	7020	11.4	
PIM-1-MeOH-L(1)-V(114)-b	4	6432	11.2	30±5
	92	3221	17.2	
	115[b)]	7165	10.1	
PIM-1-EtOH-L(1)-V(124)-a	14	5422	16.1	65±9
	73	3760	17.4	
	101	3216	17	
	125[b)]	4306	15.3	
PIM-1-EtOH-L(1)-V(120)-b	26	3364	15.4	25±2
	92	1802	22.1	
	119	1327	23.6	
	121[b)]	3712	13.3	

Note: a) Three different membranes were measured; permeability and selectivity are the average value for these 3 membranes and errors are the calculated standard deviation. The average thickness of each individual membrane is shown. b) These membranes were treated either with methanol or ethanol vapor for 8 h prior to analyzing their gas separation performance.

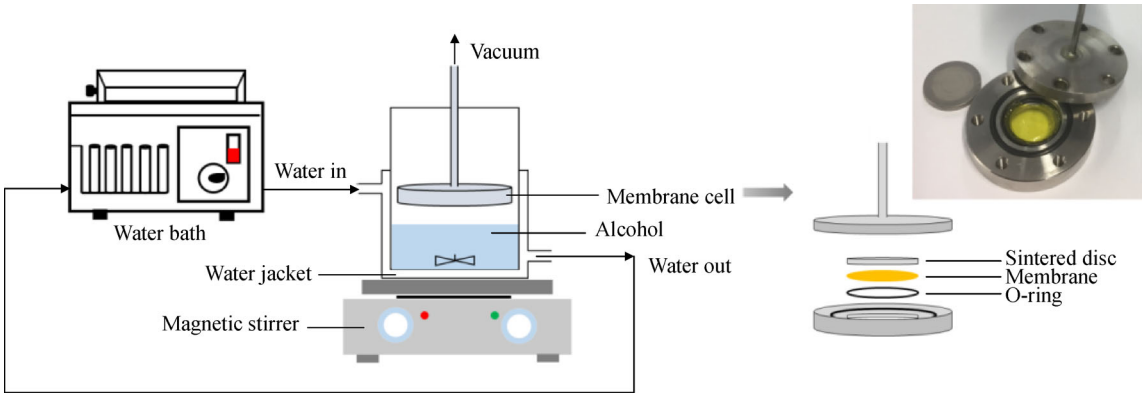

Fig. 1 Schematic of the apparatus used for the alcohol treatment of PIM-1 membranes (alcohol is kept at constant temperature by means of a water bath) and components of the membrane cell in more detail.

Fig. 1 with details on the membrane cell used. Table 1 displays the codes given to the membranes.

These membranes were treated either with liquid ethanol or liquid methanol the day after collection from casting petri dishes (day 1). Some of these membranes were further aged and some were treated with methanol or ethanol vapor after at least 114 d have passed. Aging time is the number of days after removal from petri dishes. As-cast PIM-1 membranes were also tested for comparison. The membranes were labelled using the following code: PIM-1-(alcohol used in the treatment: MeOH or EtOH)-L(day of soaking in liquid alcohol)-V(day of vapor alcohol treatment)-a or b to designate different membranes. For example membrane PIM-1-MeOH-L(1)-V(120)-a is a

membrane first soaked in methanol at day 1 and treated with methanol vapor 119 d later.

2.5 PIM-1 powder and membrane characterization

Weight-average molecular weight (M_w), number-average molecular weight (M_n) and polydispersity index (PDI) of the PIM-1 polymer was determined by gel permeation chromatography (GPC). This analysis was carried out on a Viscotek GPC mac VE 2001 instrument using tetrahydrofuran as the eluent at a flow rate of 1 mL·min^{-1} and an injection volume of 100 μL using Viscotek GPC VE2001 columns and Viscotek 3580 refractive index detector. Polystyrene standards were used for the calibration of the system.

The apparent surface area of PIM-1 was determined by Brunauer-Emmett-Teller (BET) analysis of the N_2 adsorption isotherm at 77 K. For that, PIM-1 powder was exposed to nitrogen at 77 K using a Micromeritics ASAP 2020 volumetric adsorption analyser (Micromeritics, USA). PIM-1 sample was first degassed under high vacuum at 60 °C for 12 h.

Thermogravimetric Analysis (TGA) was conducted to study the thermal stability of the PIM-1 polymer powder and the prepared films. A TGA 550 thermal analyser (TA instruments, USA) was used, heating from room temperature to 800 °C at a rate of 10 °C·min^{-1}.

The morphology of the freestanding PIM-1 membranes was studied by scanning electron microscopy (SEM) using a FEI Quanta 200 microscope (FEI, USA). The cross sectional samples were prepared via cryo-fracturing in liquid nitrogen. The samples were sputtered with Platinum nanoparticles using an Emitech sputter coater (Quorom Technologies, UK) before imaging.

The chemical structure of PIM-1 was qualitatively studied using attenuated total reflection Fourier transform infrared spectroscopy (FTIR). The spectra were acquired with an iDS Nicolet iS5 instrument (Thermo Scientific, UK), equipped with a Ge crystal over the wavenumber range of 600–4000 cm^{-1} and step size of 0.5 cm^{-1}.

2.6 Gas permeation measurements

Gas permeation measurements were performed for CO_2/CH_4 binary mixture (1:1, v:v) with a flow rate of 25 mL·min^{-1} of each gas. The feed solution was pressurized at 3 bar, while the permeate side was kept at atmospheric pressure. Helium (flow rate of 20 mL·min^{-1}) was used as a sweep gas to dilute the permeating gases and direct them to a gas chromatography system (490 micro GC, Agilent, USA) equipped with a PoraPLOT (PPU) column for the analysis of the permeate composition. The experiments were conducted at 25 °C. The gas permeability for each gas (P_i) was calculated using Eq. (1):

$$P_i = \frac{Q_i l}{A\Delta p}, \tag{1}$$

where i is either CO_2 or CH_4, Q_i is the permeate flow of gas i (cm^3(STP)·s^{-1}), l is the membrane thickness (cm), A is the effective membrane area (cm^2) and Δp is a the partial pressure difference across the membrane (cmHg) for gas component i. The results are given in barrer units (1 barrer = 10^{-10}·cm^3[STP]·cm·cm^{-2}·s^{-1}·cmHg^{-1}). The selectivity for the gas pair is calculated as the ratio of the permeabilities of the most permeable gas (P_{CO_2}) over the less permeable gas (P_{CH_4}), as shown in Eq. (2):

$$\alpha_{CO_2/CH_4} = \frac{P_{CO_2}}{P_{CH_4}}. \tag{2}$$

3 Results and discussion

3.1 PIM-1 and membrane characterization

The M_w, M_n and PDI of the PIM-1 synthesized in this study are 118800 g·mol^{-1}, 32900 g·mol^{-1} and 3.6, respectively. Figure 2(a) shows the N_2 adsorption/desorption isotherms of PIM-1 powder at 77 K. It can be observed that PIM-1 shows high N_2 uptake at very low relative pressures. The

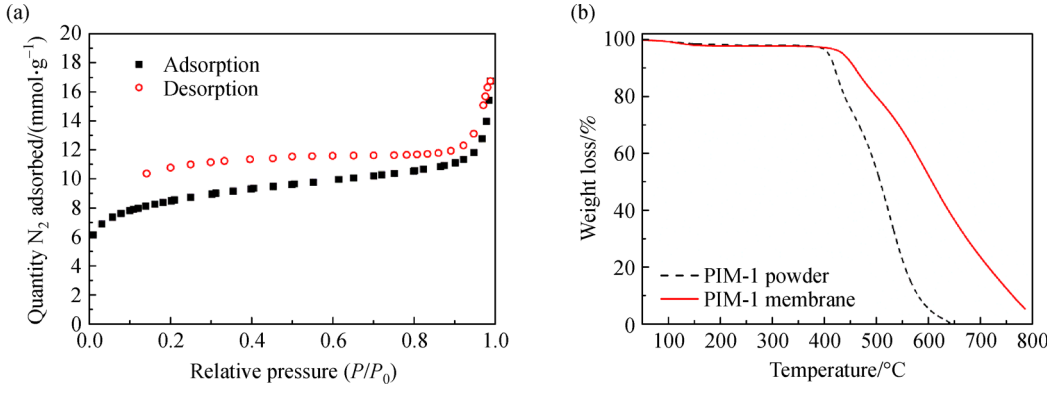

Fig. 2 (a) N_2 adsorption/desorption at 77 K for PIM-1 (square and circle symbols represent the adsorption and desorption data, respectively), and (b) TGA curves of PIM-1 powder and a PIM-1 membrane that has undergone methanol-vapor treatment.

BET surface area of PIM-1 is 657 ± 8 $m^2 \cdot g^{-1}$, which is in the typical range of values reported for PIM-1 in the literature. The thermal stability of PIM-1 powder and freestanding PIM-1 membranes was investigated through TGA. Thermogravimetric curves are shown in Fig. 2(b). It can be observed that both samples present similar thermal behavior. Below 120 °C any weight loss was due to the removal of residual solvents that might be weakly adsorbed by the material [35]. Both PIM-1 powder and PIM-1-freestanding membranes are thermally stable up to 450 °C, as the mass loss is not significant up to that temperature.

The surface and cross-section of a liquid-ethanol treated PIM-1 membrane before aging (PIM-1-EtOH-L(1)-V(120)-b), are shown in micrographs a and c in Fig. 3, respectively, and confirm the preparation of defect-free dense membranes. In addition, the cross section of an as-cast PIM-1 membrane is shown in Fig. 3(b). Some elongated deformations are present in both cross sections, with more intense creases for the as-cast membrane; these features can typically arise from the "freeze-fracture" process during sample preparation and do not indicate the presence of defects or voids within the dense membrane structure, as suggested by the gas separation performance discussed in section 3.2. The amount of residual solvent within the polymer matrix, after solvent evaporation at ambient conditions or even after vacuum treatment, influences the quality of the prepared samples; the presence of trapped solvent can lead to a more effective freezing of the polymer membrane and therefore, samples with less artificial topology, as observed in Fig. 3(c). The thickness measured for the membranes via SEM is in accordance with that measured with the micrometer.

The FTIR spectrum of an as-cast PIM-1 membrane is shown in Fig. 4 and it contains the characteristic bands and peaks that have been previously reported in the literature: aliphatic and aromatic C–H stretching (ca. 2800–3010 cm^{-1}), nitrile groups (C≡N, ca. 2240 cm^{-1}), C = C aromatic bending (ca. 1607 cm^{-1}) and C–O stretching (ca. 1000–1300 cm^{-1}) [35,36].

3.2 Evaluation of aging in PIM-1 membranes via gas permeation

Soaking membranes in polar solvents such as ethanol and methanol is often used to remove any trapped solvent or contaminants within the PIM-1 microstructure, and also to reverse the effects of aging of the films. When alcohols penetrate PIM-1 they induce swelling, polymer chains relax and this allows residual solvent to be flushed out [13]. After the removal and evaporation of the alcohol, films present an enhancement of gas permeability due to the increase of free volume. In this regard**,** the gas separation performance was studied for CO_2/CH_4 mixtures of untreated (as-cast) PIM-1 membranes, and methanol- and ethanol-treated membranes (fresh and aged ones). The CO_2 permeabilities and CO_2/CH_4 selectivities obtained for all the membranes are shown in Table 1 and plotted in permeability and selectivity graphs in Fig. 5. Untreated fresh PIM-1 membranes showed the lowest average CO_2 permeability (2755 ± 137 barrer) due to the blockage of the pores by residual casting solvent still present in the microstructure of the membranes, as has previously been reported in the literature [13,37]. When soaked in lower alcohols, the average CO_2 permeability of fresh PIM-1 membranes increased, more when methanol was used (6272 ± 142 and 4513 ± 1228 barrer for methanol and ethanol, respectively). As expected, at day 27 (ca. 4 weeks after casting), the CO_2 permeability of methanol and ethanol-treated membranes dropped by 39.3% and 29.7%, respectively. This behavior has been previously reported in the literature [21,38] and confirms the tendency to lose free volume within the polymer structure (i.e., physical aging). It is worth noting that in a previous paper from our group a very similar CO_2 permeability loss was reported, 35.9% at day 35 for freestanding PIM-1 membranes initially soaked in liquid methanol [21].

As can be observed in Table 1, liquid methanol-treated PIM-1 membrane showed higher overall CO_2 permeability right after the alcohol treatment, and also ca. 4 weeks later, as compared to ethanol-treated PIM-1 membranes. As a

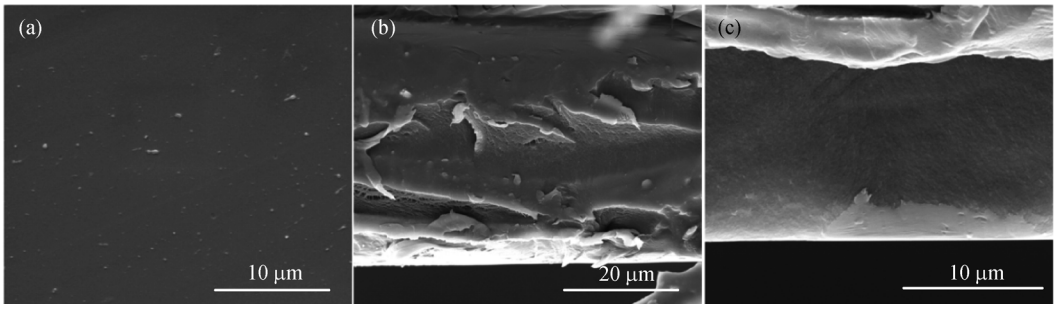

Fig. 3 SEM images of (a) the surface of an ethanol-treated PIM-1 membrane, (b) cross-section of as-cast PIM-1 membrane, and (c) cross-section of ethanol-treated membrane (PIM-1-EtOH-L(1)-V(120)-b).

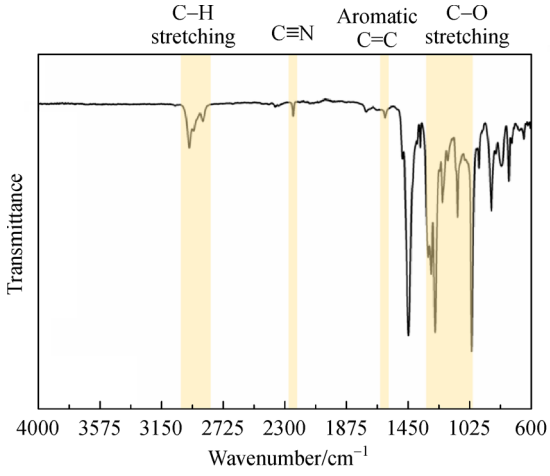

Fig. 4 FTIR spectrum of an as-cast PIM-1 freestanding membrane.

consequence of physical aging, the average CO_2 permeability dropped from 6272 ± 142 barrer down to 3810 ± 868 barrer in just 26 d, and the CO_2/CH_4 selectivity increased to 18.1 ± 4.0. These results show a superior overall performance of methanol-treated membranes compared to ethanol-treated ones, as more free volume was created upon methanol treatment. This was also observed by Mason et al. [6]. In that study, methanol-soaked aged PIM-1 films showed not only a full recovery of their gas permeabilities but also an increase compared to ethanol-treated PIM-1 films. McDermott et al. studied the effect of ethanol and methanol treatment of aged PIM-1 films on their small-angle X-ray scattering and wide-angle X-ray scattering patterns [25]. Since the porosity in PIMs, which is correlated to free volume, affects the scattering patterns, these patterns can be used to study the physical aging. Larger absolute intensity corresponds with larger porosity and, consequently, larger free volume. Their findings showed that methanol-treated PIM-1 films have larger scattering intensity compared to ethanol-treated ones, which in turn is associated with higher porosity and therefore correlated to free volume. This suggests that methanol use might be more effective as a rejuvenating procedure [25]. The effectiveness of methanol treatment in reversing the physical aging effects can also be related to the higher vapor pressure of methanol (16.96 kPa at 25 °C) compared with ethanol (7.85 kPa at 25 °C). The higher the vapor pressure, the stronger the driving force for the alcohol to evacuate the polymer structure once it is removed from the liquid, leaving additional free volume in the PIM-1. The rate of evaporation is related to the time needed for the chains to rearrange themselves in the matrix. Therefore, the higher the evaporation rate, the less time the chains have to reorient which causes an increase in free volume [11].

Vapor solvent treatment has been previously reported to enhance the mechanical properties and separation performance of electrospun membranes [39,40]. However, to the best of our knowledge, this is the first study that addresses the use of vapor solvent to reverse the effect of physical aging. CO_2 and CH_4 gas permeabilities and CO_2/CH_4 selectivity of methanol and ethanol vapor-treated membranes were monitored as a function of time. The values obtained are shown in Table 1 and also displayed in Fig. 5. It can be observed that all aged PIM-1 membranes show a decrease in gas permeability and increase in selectivity over time, similar to what is reported in other studies [9,21]. As previously explained, this is due to the loss of excess free volume and consequent rearrangement and packing of the polymer chains, and follows the trade-off between permeability and selectivity commonly seen in polymeric membranes [41]. According to Bernardo et al. [42], the effect of physical aging on the permeability, P, of aged PIM-1 membranes can be described by Eq. (3):

$$P = P_0 t^{-\beta_p} \text{ or } \log P = \log P_0 - \beta_P \log t \quad (3)$$

where P_0 is the initial permeability at $t = 1$ and β_p is the permeability aging rate constant. Figure 6 displays β_p values for PIM-1 membranes aged for ca. 4 months (last four membranes in Table 1: PIM-1-MeOH-L(1)-V(120)-a, PIM-1-MeOH-L(1)-V(114)-b, PIM-1-EtOH-L(1)-V(124)-a and PIM-1-EtOH-L(1)-V(120)-b) as a function of the square of the effective diameter (d_{eff}) of permeating gases CO_2 and CH_4 in nm^2. β_p values are very similar to those reported for PIM-1 membranes by Bernardo et al. [42] and Scholes & Kanehashi [43], which are also plotted in Fig. 6 for CO_2, CH_4 along with other gases. Only membrane PIM-1-EtOH-L(1)-V(120)-b shows higher β_p values, possibly due to the lower extent of opening up free volume with the initial ethanol soaking; it is worth noting that this membrane shows the lowest initial gas permeability of all, which upon aging for 120 d, falls below 2000 barrer.

When exposed to alcohol vapor ca. 4 months after casting, aged PIM-1 membrane PIM-1-MeOH-L(1)-V(120)-a and PIM-1-MeOH-L(1)-V(114)-b showed a full recovery of their CO_2 permeability, with values of 7020 and 7165 barrer, respectively, which are slightly above those reported initially right after the liquid-methanol treatment. On the other hand, membranes PIM-1-EtOH-L(1)-V(124)-a and PIM-1-EtOH-L(1)-V(120)-b, which were initially treated with liquid ethanol and aged for about the same period of time, also recovered their initial CO_2 permeability but the values were more scattered and ca. 50% lower. These results are again in accordance with the literature that reports the higher effectiveness of using methanol for making free volume of PIM-1 more accessible [6]. The fact that the permeability of methanol through freestanding PIM-1 membranes is approximately 3-fold the permeability of ethanol [44], also suggest a more effective treatment when the one-carbon solvent is used.

Figure 7 shows the behavior of the methanol-treated membranes PIM-1-MeOH-L(1)-V(120)-a and PIM-1-

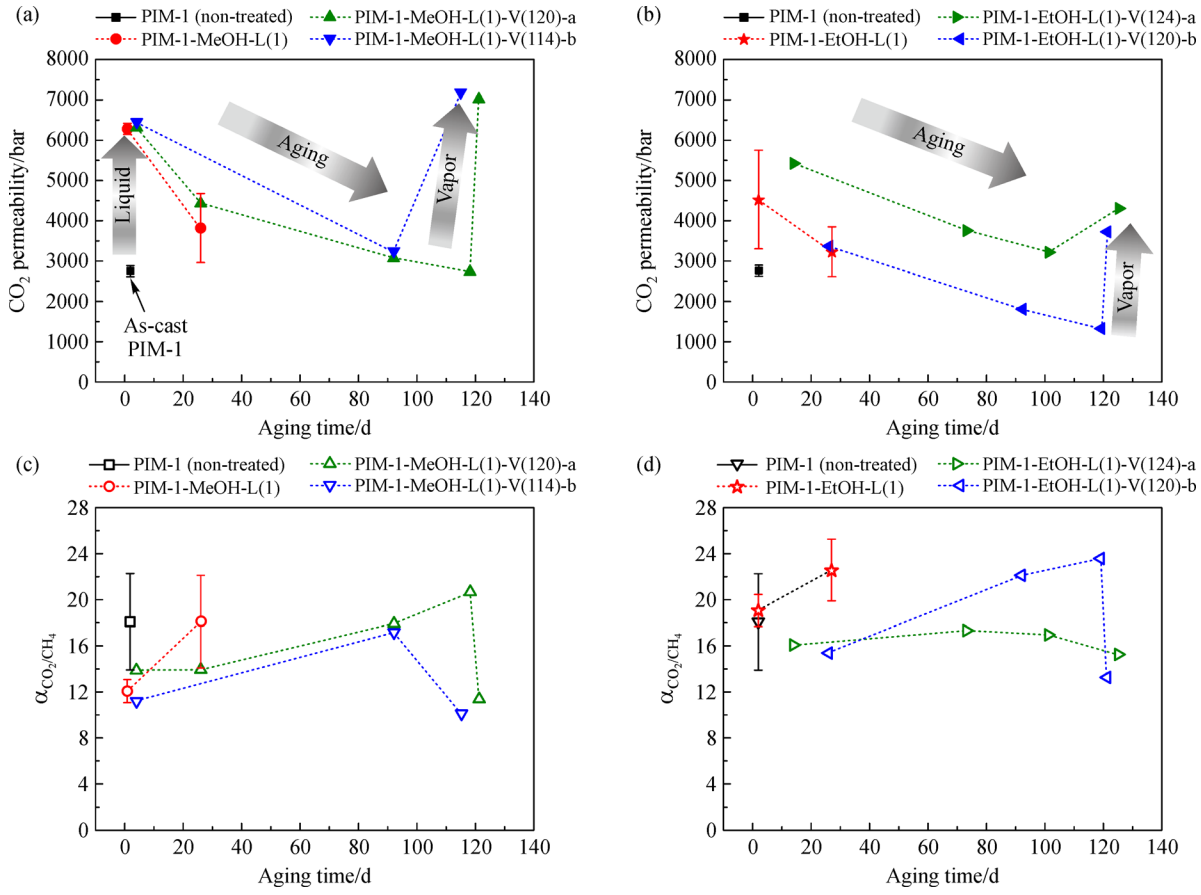

Fig. 5 CO_2 permeability of freestanding PIM-1 membranes treated with (a) methanol and (b) ethanol vapor, and CO_2/CH_4 selectivity for the same membranes treated with (c) methanol and (d) ethanol vapor. Membranes were tested using a CO_2/CH_4 binary mixture (1:1, v:v) as feed at 25 °C under a transmembrane pressure of approximately 2 bar. Values are the average permeability and selectivity for 3 membranes for those showing error bars and errors are the calculated standard deviation. PIM-1 membranes were initially treated by soaking in liquid ethanol or liquid methanol and their CO_2/CH_4 separation performance was determined at different intervals up to ca. 120 d. The membranes represented by triangles in the plot were last treated with alcohol vapor (methanol or ethanol) after ca. 4 months; the last data points give their CO_2 permeability and selectivity at that stage. All the other points in between refer to an aged state of the membrane. Filled symbols are used for CO_2 permeability values and open symbols are used for CO_2/CH_4 selectivity. Squares (■,□) correspond to PIM-1 as-cast, circles (●,○) correspond to PIM-1 membranes soaked in liquid methanol, stars (★,☆) correspond to a PIM-1 membranes soaked in liquid ethanol, and triangles (▲▼◀▶) correspond to membranes initially soaked in liquid alcohol, further aged and treated with vapor methanol or vapor ethanol after at least 114 d have passed.

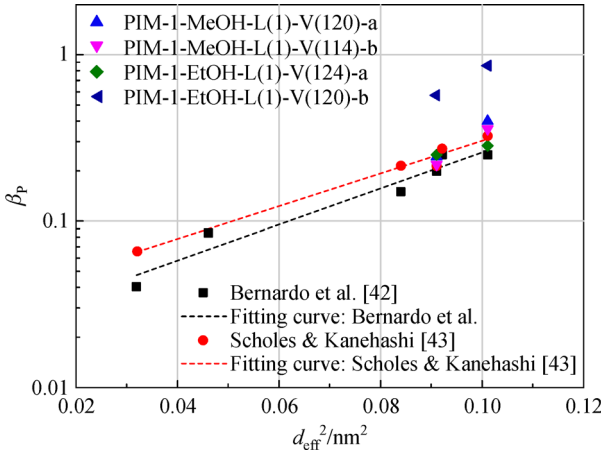

Fig. 6 Aging rate constant (β_P) as a function of the square of the effective gas diameter for PIM-1 membranes.

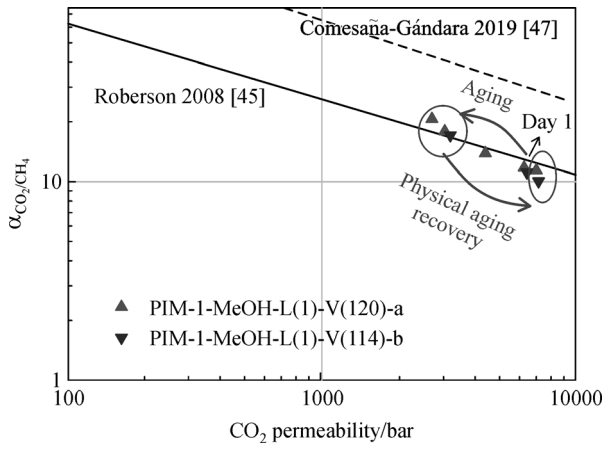

Fig. 7 Robeson plot displaying the aging behavior of PIM-1 membranes PIM-1-MeOH-L(1)-V(120)-a and PIM-1-MeOH-L (1)-V(114)-b, which were initially treated by soaking in methanol, aged for ca. 4 months (120 and 114 d, respectively) and subsequently treated with methanol vapor, for the separation of CO_2/CH_4 (1:1, v:v) mixtures. Testing was done at 25 °C and approximately 2 bar transmembrane pressure. The solid line corresponds to the revisited 2008 Robeson upper bound [45] and the dotted line represents the proposed 2019 upper bound [47]. The arrows show the aging process over the tested period and they point towards the most aged membranes.

MeOH-L(1)-V(114)-b on a CO_2/CH_4 selectivity vs CO_2 permeability double logarithmic plot. As anticipated, all PIM-1 membranes lie along the 2008 upper bound [45], since it was one of the polymers Robeson used to revisit the previous upper bound from 1991 [46]. As membranes age over time the data points move towards lower CO_2 permeability and higher CO_2/CH_4 selectivity, following the 2008 trade-off upper bound. At days 114 and 120, membranes PIM-1-MeOH-L(1)-V(120)-a and PIM-1-MeOH-L(1)-V(114)-b were exposed to methanol vapor for 8 h, respectively, and gas performance evaluated the following day. The initial performance was recovered in both cases, with CO_2 permeability values in the 7000 barrer range and CO_2/CH_4 selectivity around 11.

4 Conclusions

This study shows an effective procedure to reverse the effect of physical aging on PIM-1 membranes by exposure to vaporized alcohols (methanol or ethanol). It is anticipated that this could be done *in situ* at large scale gas separation plants. While the results obtained in this study are promising, more membranes need to be tested under different conditions, especially at higher feed pressures and at gas compositions closer to those of natural gas, in order to have a deeper and better understanding of the reversal of the physical aging effects under real operating conditions. Also, it would be useful to explore if reversibility of physical aging by means of alcohol vapor treatment would only be required upon installation of the membrane modules and after plants shutdowns; a contrasting effect of aging, i.e., plasticization, which typically occurs in glassy polymer membranes due to the presence of CO_2 at high pressures of a few tens of bar (typical operation conditions of sweetening of natural gas), most likely will impede physical aging during membrane operation.

These findings suggest the effectiveness of the vapor methanol treatment as a ‘rejuvenation’ process which may bring the use of PIM-1 membranes in industrial applications one step closer.

Acknowledgements Faiz Almansour is grateful to the Department of Research & Development, Saudi Aramco for funding and supporting his Ph.D. studies. M. Alberto is grateful to EPSRC for funding under the research grant number EP/S032258/1 and R. Bhavsar to EPSRC under grant number EP/M001342/1.

References

1. Low Z X, Budd P M, McKeown N B, Patterson D A. Gas permeation properties, physical aging, and its mitigation in high free volume glassy polymers. Chemical Reviews, 2018, 118(12): 5871–5911
2. Budd P M, Ghanem B S, Makhseed S, McKeown N B, Msayib K J, Tattershall C E. Polymers of intrinsic microporosity (PIMs): robust, solution-processable, organic nanoporous materials. Chemical Communications, 2004, (2): 230–231
3. Budd P M, McKeown N B, Fritsch D. Polymers of intrinsic microporosity (PIMs): high free volume polymers for membrane applications. Macromolecular Symposia, 2006, 245-246(1): 403–405
4. Kim S, Lee Y M. Rigid and microporous polymers for gas separation membranes. Progress in Polymer Science, 2015, 43: 1–32
5. Du N, Cin M M D, Pinnau I, Nicalek A, Robertson G P, Guiver M D. Azide-based cross-linking of polymers of intrinsic microporosity (PIMs) for condensable gas separation. Macromolecular Rapid Communications, 2011, 32(8): 631–636
6. Mason C R, Maynard-Atem L, Heard K W J, Satilmis B, Budd P M, Friess K, Lanc MBernardo P, Clarizia G, Jansen J C. Enhancement of CO_2 affinity in a polymer of intrinsic microporosity by amine modification. Macromolecules, 2014, 47(3): 1021–1029
7. Bakhtin D S, Kulikov L A, Legkov S A, Khotimskiy V S, Levin I S,

Borisov I L, Maksimov A L, Volkov V V, Karakhanov E A, Volkov A V. Aging of thin-film composite membranes based on PTMSP loaded with porous aromatic frameworks. Journal of Membrane Science, 2018, 554: 211–220

8. Harms S, Rätzke K, Faupel F, Chaukura N, Budd P M, Egger W, Ravelli L. Aging and free volume in a polymer of intrinsic microporosity (PIM-1). Journal of Adhesion, 2012, 88(7): 608–619
9. Tiwari R R, Jin J, Freeman B D, Paul D R. Physical aging, CO_2 sorption and plasticization in thin films of polymer with intrinsic microporosity (PIM-1). Journal of Membrane Science, 2017, 537: 362–371
10. Nagai K, Nakagawa T. Effects of aging on the gas permeability and solubility in poly(1-trimethylsilyl-1-propyne) membranes synthesized with various catalysts. Journal of Membrane Science, 1995, 105(3): 261–272
11. Jue M L, McKay C S, McCool B A, Finn M G, Lively R P. Effect of nonsolvent treatments on the microstructure of PIM-1. Macromolecules, 2015, 48(16): 5780–5790
12. Swaidan R, Ghanem B, Litwiller E, Pinnau I. Physical aging, plasticization and their effects on gas permeation in “rigid” polymers of intrinsic microporosity. Macromolecules, 2015, 48 (18): 6553–6561
13. Budd P M, McKeown N B, Ghanem B S, Msayib K J, Fritsch D, Starannikova L, Belov N, Sanfirova O, Yampolskii Y, Shantarovich V. Gas permeation parameters and other physicochemical properties of a polymer of intrinsic microporosity: polybenzodioxane PIM-1. Journal of Membrane Science, 2008, 325(2): 851–860
14. Bushell A F, Attfield M P, Mason C R, Budd P M, Yampolskii Y, Starannikova L, Rebrov A, Bazzarelli F, Bernardo P, Carolus Jansen J, Lanč M, Friess K, Shantarovich V, Gustov V, Isaeva V. Gas permeation parameters of mixed matrix membranes based on the polymer of intrinsic microporosity PIM-1 and the zeolitic imidazolate framework ZIF-8. Journal of Membrane Science, 2013, 427: 48–62
15. Carta M, Malpass-Evans R, Croad M, Rogan Y, Jansen J C, Bernardo P, Bazzarelli F, McKeown N B. An efficient polymer molecular sieve for membrane gas separations. Science, 2013, 339 (6117): 303–307
16. Carta M, Croad M, Malpass-Evans R, Jansen J C, Bernardo P, Clarizia G, Friess K, Lanč M, McKeown N B. Triptycene induced enhancement of membrane gas selectivity for microporous Tröger’s base polymers. Advanced Materials, 2014, 26(21): 3526–3531
17. Rose I, Carta M, Malpass-Evans R, Ferrari M C, Bernardo P, Clarizia G, Jansen J C, McKeown N B. Highly permeable benzotriptycene-based polymer of intrinsic microporosity. ACS Macro Letters, 2015, 4(9): 912–915
18. Ma X, Mukaddam M, Pinnau I. Bifunctionalized intrinsically microporous polyimides with simultaneously enhanced gas permeability and selectivity. Macromolecular Rapid Communications, 2016, 37(11): 900–904
19. Song Q, Cao S, Pritchard R H, Ghalei B, Al-Muhtaseb S A, Terentjev E M, Cheetham A K, Sivaniah E. Controlled thermal oxidative crosslinking of polymers of intrinsic microporosity towards tunable molecular sieve membranes. Nature Communications, 2014, 5(1): 4813
20. Li F Y, Chung T S. Physical aging, high temperature and water vapor permeation studies of UV-rearranged PIM-1 membranes for advanced hydrogen purification and production. International Journal of Hydrogen Energy, 2013, 38(23): 9786–9793
21. Alberto M, Bhavsar R, Luque-Alled J M, Vijayaraghavan A, Budd P M, Gorgojo P. Impeded physical aging in PIM-1 membranes containing graphene-like fillers. Journal of Membrane Science, 2018, 563: 513–520
22. Bhavsar R S, Mitra T, Adams D J, Cooper A I, Budd P M. Ultrahigh-permeance PIM-1 based thin film nanocomposite membranes on PAN supports for CO_2 separation. Journal of Membrane Science, 2018, 564: 878–886
23. Yong W F, Kwek K H A, Liao K S, Chung T S. Suppression of aging and plasticization in highly permeable polymers. Polymer, 2015, 77: 377–386
24. Horn N R, Paul D R. Carbon dioxide plasticization of thin glassy polymer films. Polymer, 2011, 52(24): 5587–5594
25. McDermott A G, Budd P M, McKeown N B, Colina C M, Runt J. Physical aging of polymers of intrinsic microporosity: a SAXS/WAXS study. Journal of Materials Chemistry. A, Materials for Energy and Sustainability, 2014, 2(30): 11742–11752
26. Hill A J, Pas S J, Bastow T J, Burgar M I, Nagai K, Toy L G, Freeman B D. Influence of methanol conditioning and physical aging on carbon spin-lattice relaxation times of poly(1-trimethylsilyl-1-propyne). Journal of Membrane Science, 2004, 243(1): 37–44
27. Razali M, Didaskalou C, Kim J F, Babaei M, Drioli E, Lee Y M, Szekely G. Exploring and exploiting the effect of solvent treatment in membrane separations. ACS Applied Materials & Interfaces, 2017, 9(12): 11279–11289
28. Jimenez Solomon M F, Bhole Y, Livingston A G. High flux hydrophobic membranes for organic solvent nanofiltration (OSN)—interfacial polymerization, surface modification and solvent activation. Journal of Membrane Science, 2013, 434: 193–203
29. Gorgojo P, Jimenez-Solomon M F, Livingston A G. Polyamide thin film composite membranes on cross-linked polyimide supports: improvement of RO performance via activating solvent. Desalination, 2014, 344: 181–188
30. Zhao Y, Yuan Q. Effect of membrane pretreatment on performance of solvent resistant nanofiltration membranes in methanol solutions. Journal of Membrane Science, 2006, 280(1): 195–201
31. Shukla R, Cheryan M. Performance of ultrafiltration membranes in ethanol-water solutions: effect of membrane conditioning. Journal of Membrane Science, 2002, 198(1): 75–85
32. Penha F M, Rezzadori K, Proner M C, Zanatta V, Zin G, Tondo D W, Vladimir de Oliveira J, Petrus J C C, Di Luccio M. Influence of different solvent and time of pre-treatment on commercial polymeric ultrafiltration membranes applied to non-aqueous solvent permeation. European Polymer Journal, 2015, 66: 492–501
33. Nguyen Q T, Favre E, Ping Z H, Néel J. Clustering of solvents in membranes and its influence on membrane transport properties. Journal of Membrane Science, 1996, 113(1): 137–150
34. Du N, Song J, Robertson G P, Pinnau I, Guiver M D. Linear high molecular weight ladder polymer via fast polycondensation of 5,5′,6,6′-tetrahydroxy-3,3,3′,3′-tetramethylspirobisindane with 1,4-dicyanotetrafluorobenzene. Macromolecular Rapid Communications, 2008, 29(10): 783–788
35. Satilmis B, Budd P M. Base-catalysed hydrolysis of PIM-1: amide

versus carboxylate formation. RSC Advances, 2014, 4(94): 52189–52198

36. Hao L, Liao K S, Chung T S. Photo-oxidative PIM-1 based mixed matrix membranes with superior gas separation performance. Journal of Materials Chemistry. A, Materials for Energy and Sustainability, 2015, 3(33): 17273–17281
37. Zhang L, Fang W, Jiang J. Effects of residual solvent on membrane structure and gas permeation in a polymer of intrinsic microporosity: insight from atomistic simulation. Journal of Physical Chemistry C, 2011, 115(22): 11233–11239
38. Mitra T, Bhavsar R S, Adams D J, Budd P M, Cooper A I. PIM-1 mixed matrix membranes for gas separations using cost-effective hypercrosslinked nanoparticle fillers. Chemical Communications, 2016, 52(32): 5581–5584
39. Abd Halim N S, Wirzal M D H, Bilad M R, Md Nordin N A H, Adi Putra Z, Sambudi N S, Mohd Yusoff A R. Improving performance of electrospun nylon 6,6 nanofiber membrane for produced water filtration via solvent vapor treatment. Polymers, 2019, 11(12): 2117
40. Rianjanu A, Kusumaatmaja A, Suyono E A, Triyana K. Solvent vapor treatment improves mechanical strength of electrospun polyvinyl alcohol nanofibers. Heliyon, 2018, 4(4): e00592
41. Brunetti A, Cersosimo M, Kim J S, Dong G, Fontananova E, Lee Y M, Drioli E, Barbieri G. Thermally rearranged mixed matrix membranes for CO_2 separation: an aging study. International Journal of Greenhouse Gas Control, 2017, 61: 16–26
42. Bernardo P, Bazzarelli E, Tasselli F, Clarizia G, Mason C R, Maynard-Atem L, Budd P M, Lanc M, Pilnacek K, Vopicka O, Friess K, Fritsch D, Yampolskii Y P, Shantarovich V, Jansen J C. Effect of physical aging on the gas transport and sorption in PIM-1 membranes. Polymer, 2017, 113: 283–294
43. Scholes C A, Kanehashi S. Polymer of intrinsic microporosity (PIM-1) membranes treated with supercritical CO_2. Membranes, 2019, 9(3): 1–12
44. Adymkanov S V, Yampol'skii Y P, Polyakov A M, Budd P M, Reynolds K J, McKeown N B, Msayib K J. Pervaporation of alcohols through highly permeable PIM-1 polymer films. Polymer Science, Series A, 2008, 50(4): 444–450
45. Robeson L M. The upper bound revisited. Journal of Membrane Science, 2008, 320(1): 390–400
46. Robeson L M. Correlation of separation factor versus permeability for polymeric membranes. Journal of Membrane Science, 1991, 62 (2): 165–185
47. Comesaña-Gándara B, Chen J, Bezzu C G, Carta M, Rose I, Ferrari M C, Esposito E, Fuoco A, Jansen J C, McKeown N B. Redefining the Robeson upper bounds for CO_2/CH_4 and CO_2/N_2 separations using a series of ultrapermeable benzotriptycene-based polymers of intrinsic microporosity. Energy & Environmental Science, 2019, 12 (9): 2733–2740